Full pf shell model study of A=48 nuclei

E. Caurier and A. P. Zuker
Groupe de Physique Théorique, Centre de Recherches Nucléaires, Institut National de Physique Nucléaire et de Physique des Particles, Centre National de la Recherche Scientifique, Université Louis Pasteur Boîte Postale 20, F-67037 Strasbourg-Cedex, France

A. Poves and G. Martínez-Pinedo
Departamento de Física Teórica C-XI, Universidad Autónoma de Madrid, E-28049 Madrid, Spain
(Received 16 December 1993)

Exact diagonalizations with a minimally modified realistic force lead to detailed agreement with measured level schemes and electromagnetic transitions in ^{48}Ca, ^{48}Sc, ^{48}Ti, ^{48}V, ^{48}Cr, and ^{48}Mn. Gamow-Teller strength functions are systematically calculated and reproduce the data to within the standard quenching factor. Their fine structure indicates that fragmentation makes much strength unobservable. As a by-product, the calculations suggest a microscopic description of the onset of rotational motion. The spectroscopic quality of the results provides strong arguments in favor of the general validity of monopole corrected realistic forces, which is discussed.

PACS number(s): 21.10.−k, 27.40.+z, 21.60.Cs, 23.40.−s

I. INTRODUCTION

Exact diagonalizations in a full major oscillator shell are the privileged tools for spectroscopic studies up to $A \approx 60$. The total number of states —2^d with d = 12, 24, and 40 in the p, sd, and pf shells, respectively— increases so fast that three generations of computers and computer codes have been necessary to move from $n = 4$ to $n = 8$ in the pf shell, i.e., from four to eight valence particles, which is our subject.

A peculiarity of the pf shell is that a minimally modified realistic interaction has been waiting for some 15 years to be tested in exact calculations *with a sufficiently large number of particles*, and as we shall explain in due course $n = 8$ happens to be the smallest for which success was practically guaranteed. In the test, spectra and electromagnetic transitions will be given due place but the emphasis will go to processes governed by spin operators: beta decays, (p, n) and (n, p) reactions. They are interesting—perhaps fascinating is a better word— on two counts. They demand a firm understanding of not simply a few, but very many levels of given J and they raise the problem of quenching of the Gamow-Teller (GT) strength.

As by-products, the calculations provide clues on rotational motion and some helpful indications about possible truncations of the spaces. The paper is arranged as follows.

Section II contains the definition of the operators. Some preliminary comments on the interaction are made.

In each of the following six sections, next to the name of the nucleus to which it is devoted, the title contains a comment directing attention to a point of interest. The one for ^{48}Ca is somewhat anomalous.

In Sec. IX, the evidence collected on GT strength is analyzed. Our calculations reproduce the data once we adopt a quenching factor of $(0.77)^2$. We shall refer to it as "standard" because it seems to represent some consensus among workers in the field [1]. The fine structure of the strength function indicates that fragmentation could make impossible the observation of many peaks. Several experimental checks are suggested.

In Sec. X we examine the following question: *Why, in the sd shell, have phenomenologically fitted matrix elements been so far necessary to yield results of a quality comparable with the ones we obtain here with a minimally modified realistic interaction?* The short answer is that *monopole* corrected realistic forces are valid in general, but the fact is easier to detect in the pf shell.

Section XI contains a brief note on binding energies. In Sec. XII we conclude.

The rest of the Introduction is devoted to a point of notation, a review of previous work, and a word on the diagonalizations.

Notations. Throughout the paper f stands for $f_{7/2}$ (except of course when we speak of the pf shell) and r, generically, for any or all of the other subshells $(p_{1/2}\, p_{3/2}\, f_{5/2})$. Spaces of the type

$$f^{n-n_0}r^{n_0} + f^{n-n_0-1}r^{n_0+1} + \cdots + f^{n-n_0-t}r^{n_0+t} \quad (1)$$

represent possible truncations: n_0 is different from zero if more than eight neutrons are present and when $t = n-n_0$ we have the full space $(pf)^n$ for A = 40 + n.

Bibliographical note. The characteristic that makes the pf shell unique in the periodic table is that at $t = 0$ we already obtain a very reasonable model space, as demonstrated in the f^n case (i.e., $n_0 = 0$) by Ginocchio and French [2] and McCullen, Bayman, and Zamick [3] (MBZ in what follows). The $n_0 \neq 0$ nuclei are technically more demanding but the $t = 0$ approximation is again excellent (Horie and Ogawa [4]).

The first systematic study of the truncation hierarchy was undertaken by Pasquini and Zuker [5,6] who found that $t = 1$ has beneficial effects, and $t = 2$ may be dangerous and even nonsensical, while $t = 3$ restored sense in the only nontrivial case tractable at the time (^{56}Ni).

TABLE I. m-scheme and maximal JT dimensions in the full pf shell.

	^{48}Ca	^{48}Sc	^{48}Ti	^{48}V	^{48}Cr
m scheme	12 022	139 046	634 744	1 489 168	1 963 461
$J\ T$	4 4	4 3	4 2	5 1	4 0
	1 755	17 166	63 757	106 225	58 219

This seems to be generally a fair approximation, and the topic will be discussed as we proceed.

Much work on $n_0 \neq 0$ nuclei with $t = 1$ and 2 spaces was done by the groups in Utrecht and Tokyo [7–12].

For the Ca isotopes high t and even full space diagonalizations have been possible [13,14].

Exact calculations for $n \leq 4$ are due to McGrory [15], and some $n = 5$ nuclei were studied by Cole [16] and by Richter *et al.* in a paper in which two sets of interaction matrix elements are constructed [17].

For $n = 6$, 7, and 8 the only exact results reported so far are those of the authors on the magnetic properties of the Ti isotopes [18], and the double β decay calculations of ^{48}Ca by Ogawa and Horie [19], the authors [20], and Engel, Haxton, and Vogel [21]. The MBZ model has been reviewed in an appendix to Pasquini's thesis [5] and by Kutschera, Brown, and Ogawa [22]. Its success suggested the implementation of a perturbative treatment in the full pf shell by Poves, Pasquini, and Zuker [23,24].

All the experimental results for which no explicit credit is given come from the recent compilation of Burrows for A=48 [25].

The diagonalizations are performed in the m scheme using a fast implementation of the Lanczos algorithm through the code ANTOINE [26]. Some details may be found in Ref. [27]. The strength functions are obtained through Whitehead's prescription [28], explained and illustrated in Refs. [18,20,29] (and Sec. IX). The m scheme and maximal JT dimensions of the nuclei analyzed are given in Table I. To the best of our knowledge they are the largest attained so far.

II. INTERACTION AND OTHER OPERATORS

A characteristic of this paper is that it is the first that demonstrates in some detail the possibility—or even the need—to use minimally modified realistic interactions. The problem encountered by these forces, in particular Kuo-Brown (KB) forces [30], is that spectra deteriorate rapidly as the number of particles increases. In ^{49}Ca, for instance, below 4 MeV the calculated levels are twice more numerous than the observed ones. In ^{56}Ni the $f^{12}r^4$ configurations come some 5 MeV below the f^{16} closed shell. The most interesting result of Refs. [5,6] was that these spectroscopic catastrophes could be cured by the simple modification (KB′ in [5,6])

$$V^T_{fr}(\mathrm{KB1}) = V^T_{fr}(\mathrm{KB}) - (-)^T\ 300\,\mathrm{keV}, \tag{2}$$

where V^T_{fr} are the centroids, defined for any two shells by

$$V^T_{ij} = \frac{\sum_J (2J+1) W^{JT}_{ijij}}{\sum_J (2J+1)}, \tag{3}$$

where the sums run over Pauli allowed values if $i = j$, and W^{JT}_{ijij} are two-body matrix elements. For $i, j \equiv r$, no defects can be detected until much higher in the pf region. On the contrary, the calculations are quite sensitive to changes in W^{JT}_{ffff} but the only ones that are compulsory affect the centroids and it is the binding energies that are sensitive to them:

$$V^0_{ff}(\mathrm{KB1}) = V^0_{ff}(\mathrm{KB}) - 350\ \mathrm{keV},$$
$$V^1_{ff}(\mathrm{KB1}) = V^1_{ff}(\mathrm{KB}) - 110\ \mathrm{keV}. \tag{4}$$

Equations (2) and (4) define the KB1 interaction. These modifications are minimal in that the bad behavior of the centroids reflects the bad saturation properties of the realistic potentials: If we do not accept corrections to the centroids, we have no realistic interaction.

Once this fundamental problem is solved, minor ones remain. The interaction we use in the paper, KB3, was defined in Ref. [24] as

$$W^{J0}_{ffff}(\mathrm{KB3}) = W^{J0}_{ffff}(\mathrm{KB1}) - 300\,\mathrm{keV} \text{ for } J = 1, 3,$$
$$W^{21}_{ffff}(\mathrm{KB3}) = W^{21}_{ffff};(\mathrm{KB1}) - 200\,\mathrm{keV}, \tag{5}$$

while the other matrix elements are modified so as to keep the centroids (4).

These very mild changes were made to improve the spectroscopy of some nuclei at the beginning of the pf shell. After the calculations were completed and analyzed, we came to regret the choice of KB3, since it is hard to see the improvements it brings—if any—over KB1 in A=48, and it distracts attention from the truly important—minimal—corrections. However, KB3 raises some interesting questions that will be discussed in Sec. X.

In what follows, and unless specified otherwise, we use (i) harmonic oscillator wave functions with $b = 1.93$ fm; (ii) bare electromagnetic factors in $M1$ transitions; effective charges of $1.5e$ for protons and $0.5e$ for neutrons in the electric quadrupole transitions and moments; (iii) Gamow-Teller (GT) strength defined through

$$B(\mathrm{GT}) = \kappa^2 \langle \sigma\tau \rangle^2, \qquad \langle \sigma\tau \rangle = \frac{\langle f || \sum_k \sigma^k t^k_\pm || i \rangle}{\sqrt{2J_i + 1}}, \tag{6}$$

where the matrix element is reduced with respect to the spin operator only (Racah convention [31]) and κ is the axial to vector ratio for GT decays,

$$\kappa = (g_A/g_V)_{\mathrm{eff}} = 0.77 (g_A/g_V)_{\mathrm{bare}} = 0.963(7); \tag{7}$$

(iv) for Fermi decays we have

$$B(F) = \langle \tau \rangle^2, \qquad \langle \tau \rangle = \frac{\langle f || \sum_k t^k_\pm || i \rangle}{\sqrt{2J_i + 1}}; \tag{8}$$

(v) half-lives $T_{1/2}$ are found through

$$(f_A + f^\epsilon)\ T_{1/2} = \frac{6170 \pm 4}{(f_V/f_A) B(F) + B(\mathrm{GT})}. \tag{9}$$

We follow Ref. [32] in the calculation of the f_A and f_V integrals and Ref. [33] for f^ϵ. The experimental energies are used.

III. ^{48}Ca, ERRATUM

In Fig. 1 we compare calculated and experimental levels. Except for the lowest 2^+ state the agreement is good and the first excited 0^+ is certainly an intruder.

The calculated $M1$ strength is found in a triplet (not shown) at excitation energies of 9.82, 10.06, and 10.23 MeV with $B(M1)$ values of $0.39\mu_N^2$, $6.17\mu_N^2$, and $1.81\,\mu_N^2$, respectively, which nearly exhaust the sum rule of $8.96\mu_N^2$. The total observed strength between 7.5 and 12.5 MeV is $(5.2\pm0.5)\mu_N^2$. It is dominated by a majestic peak at 10.2 MeV ($3.9\mu_N^2$) and otherwise fragmented among some 20 states; below 11.7 MeV there are 14 peaks where the calculation only produced 8. The observed to calculated ratio $5.2/8.96=(0.76)^2$ is very much the standard value for spinlike operators.

The $E2$ rates

$$B(E2,4^+\rightarrow 2^+)=2.65\,e^2\ \mathrm{fm}^4,$$
$$B(E2,2^+\rightarrow 0^+)=10.2\,e^2\ \mathrm{fm}^4, \qquad (10)$$

agree reasonably with the experimental values

$$B(E2,4^+\rightarrow 2^+)_{\mathrm{expt}}=1.89e^2\ \mathrm{fm}^4,$$
$$B(E2,2^+\rightarrow 0^+)_{\mathrm{expt}}=17.2e^2\ \mathrm{fm}^4, \qquad (11)$$

but definitely suggest that something is missing in a strict $0\hbar\omega$ calculation.

In Ref. [20] we studied 2ν double β decay of ^{48}Ca and calculated the strength functions for the associated processes $^{48}\mathrm{Ca}(p,n)^{48}\mathrm{Sc}$ and $^{48}\mathrm{Ti}(n,p)^{48}\mathrm{Sc}$, and for the latter we have to offer the following:

Erratum. The total $^{48}\mathrm{Ti}(n,p)^{48}\mathrm{Sc}$ strength in Ref. [20] is missing a factor of 3/2. Hence the ^{48}Ca 2ν double β decay half-life has to be multiplied by a factor of 2/3 to yield $T_{1/2}=3.7\times10^{19}$ yr.

IV. ^{48}Sc, THE FAMOUS SEVEN

The $J=1-7$, $T=3$, multiplet of f^8 states in ^{48}Sc can be related to f^2 states in ^{42}Sc through a Racah coefficient (the Pandya-Talmi transformation). The operation is successful enough to have become a textbook example. There are some discrepancies that are removed by a t=1 truncation, which provided early evidence of the quality of the realistic forces [6]. These levels change very little in going from t=1 to perturbative [23,24] and then to the exact results, but they are quite sensitive to changes in the W_{ffff} matrix elements. In all the other nuclei the situation is reversed and Fig. 2 provides the *only* example of an exact calculation that does not bring an improvement over the approximate ones. Note however that the agreement with the data is definitely good, and extends to three levels at around 2 MeV that do not belong to the multiplet. Below 2.5 MeV there are a couple of 2^+ states with no calculated counterparts, i.e., intruders. A more complete view of the density of intruders comes from Table II, where we have listed the 9 calculated 1^+ levels below 6 MeV against 13 experimental candidates [34]. Immediately above 6 MeV, diagonalizations yield level spacings of 100 keV. The number of intruders will also grow fast and one to one identifications become meaningless because the number of levels that can be observed becomes a small fraction of those present. Note that even some of the calculated states in Table II may have escaped detection (e.g., the one at 5.23 MeV).

^{48}Sc decays to ^{48}Ti via the doublet of 6^+ states at 3.33 and 3.51 MeV. The measured half-life, log ft values, and branching ratios are

$$T_{1/2}=43.7\ \mathrm{h},$$
$$\log ft(6_1^+)=5.53,\ \ \%\beta=90.7\%, \qquad (12)$$
$$\log ft(6_2^+)=6.01,\ \ \%\beta=9.3\%,$$

while the calculated ones read

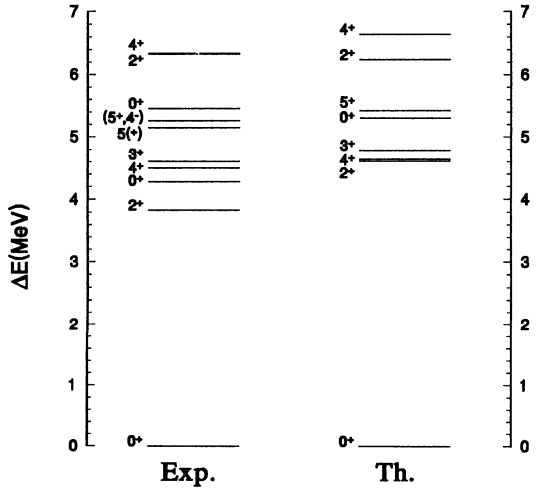

FIG. 1. Experimental and theoretical energy levels of ^{48}Ca.

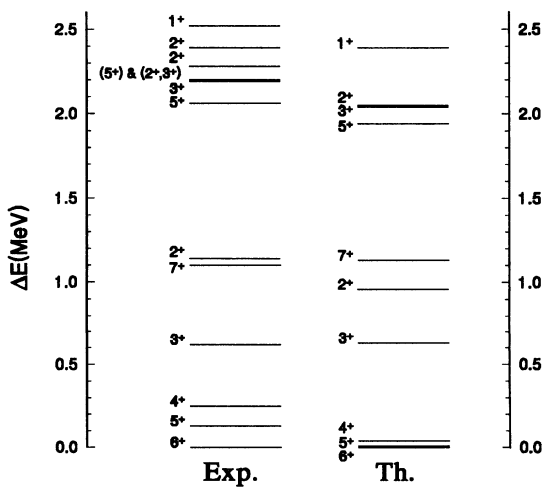

FIG. 2. Experimental and theoretical energy levels of ^{48}Sc.

TABLE II. 1^+ states in ^{48}Sc. Energies in MeV.

Expt.	2.52	2.98	3.06	3.16	3.26	3.71	4.00	4.18	4.32	4.68	4.78	5.45	5.74
Theor.	2.39	2.91			3.46		3.95		4.49	4.67	5.23	5.49	5.79

$$T_{1/2} = 29.14 \text{ h},$$
$$\log ft(6_1^+) = 5.34, \ \%\beta = 96\%, \tag{13}$$
$$\log ft(6_2^+) = 6.09, \ \%\beta = 4\%.$$

We have here a first example of the extreme sensitivity of the half-lives to effects that are bound to produce very minor changes in other properties that are satisfactorily described, such as those of the 6^+ doublet (see next section).

We have also calculated the total GT^+ and GT^- strengths for different truncations and for the complete calculations. When we use the truncation level t in the parent nucleus we use the $t+1$ level in the daughter in order to satisfy the $3(N-Z)$ sum rule. The results in units of the sum rule are the following:

t_{parent}	t_{daughter}	GT^-	GT^+
0	1	19.71	1.71
1	2	19.27	1.27
2	3	18.94	0.94
3	4	18.88	0.88
Full	Full	18.85	0.85

There is a factor of 2 reduction of the GT^+ strength between the MBZ and the full result. The $t_{\text{parent}} = 3$ result is already very close to that of the full calculation, while a $t_{\text{daughter}} = 2$ calculation is far from the exact result. We shall see that the same is true in all the A=48 nuclei.

V. ^{48}Ti, INTRINSIC STATES

Experimentally this is the richest of the A=48 nuclei. The lines in Fig. 3 connect theoretical levels (to the right) with observed ones (to the left). The agreement, which would be perfect if all lines were horizontal, is nevertheless quite good: The rms deviation for the 33 excited states is 110 keV. Dots correspond to the first intruders detected for a given J value.

Tables III and IV contain the information on $E2$ and $M1$ transitions, to which we may add the magnetic moment of the first 2^+ state, calculated to be $\mu(2^+) = 0.43\mu_N$, lowish with respect to the measured $\mu(2^+) = 0.86\,(38)\mu_N$ and $\mu(2^+) = 1.12\,(22)\mu_N$ [35].

There are very few discrepancies between the exact calculations $(fp)^8$ and the data, and they are hardly significant. For the f^8 calculations the agreement is fairly good for the $M1$ rates, less so for $E2$ [note in particular the spectacular case of $B(E2, 6^+_{1,2} \to 4^+_1)$]. The exact results build enough quadrupole coherence with standard effective charges but the truly important difference with the t=0 calculations is shown in Table V, where we have collected the intrinsic quadrupole moment Q_0, extracted from the spectroscopic ones through

$$Q_0 = \frac{(J+1)\,(2J+3)}{3K^2 - J(J+1)}\, Q_{\text{spec}}(J), \tag{14}$$

setting $K = 0$. For the exact calculations, Q_0 is also extracted through the rotational model prescription

$$B(E2, J \to J-2) = \frac{5}{16\pi}\, e^2 |\langle JK20|J-2, K\rangle|^2\, Q_0^2. \tag{15}$$

The wrong sign for the quadrupole moment is a characteristic of the $t = 0$ calculations. The exact results check well with the known experimental value for the 2^+ but they do much more: The curious mixture of signs and sizes coming out of f^8 becomes a fairly large and constant number for $(pf)^8$.

Although we cannot speak of rotational motion—which demands a truly constant Q_0 and a $J(J+1)$ spectrum—*we are certainly in the presence of a well defined prolate intrinsic structure.*

This buildup of quadrupole coherence is almost entirely due to mixing with the $p_{3/2}$ orbit, as seen from the results for the $(f_{7/2}\, p_{3/2})^8$ space.

The strength function for ^{48}Ti$(n,p)^{48}$Sc can be found in Ref. [20] (remember the erratum though) and Ref. [18] contains a study of the (p,p') and (e,e') processes and an analysis of the orbital, spin, and $M1$ strengths. The missing piece of information, ^{48}Ti$(p,n)^{48}$V, is found in Figs. 4 and 5, for $t = 1$ and exact calculations. They show

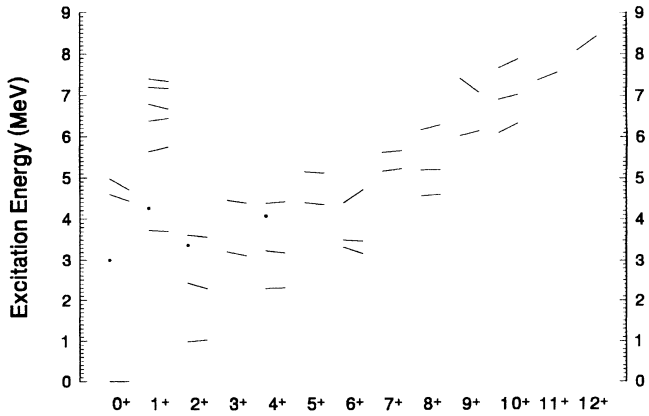

FIG. 3. Experimental and theoretical energy level of ^{48}Ti. The left side of the lines corresponds to the experimental value; the right side corresponds to the theoretical one. The isolated points are intruder states not included in our valence space.

TABLE III. ^{48}Ti $E2$ transitions, $B(E2)$ in e^2 fm^4. $f^8(^{42}\mathrm{Sc})$ is a t=0 calculation with W_{ffff} matrix elements taken from the spectrum of ^{42}Sc.

J_n^π(i)	J_m^π(f)	Expt.	$(fp)^8$	$f^8(^{42}\mathrm{Sc})$
2_1^+	0_1^+	142 ± 6	92.1	52.9
4_1^+	2_1^+	111 ± 20	136.6	65.8
2_2^+	2_1^+	104 ± 104	36.0	45.2
2_2^+	0_1^+	13 ± 2	20.3	6.6
2_3^+	0_1^+	22 ± 6	4.3	0.2
6_1^+	4_1^+	52 ± 5	54.8	39.3
6_2^+	4_1^+	56 ± 25	55.5	0.7
6_3^+	4_1^+	75 ± 30	34.1	29.8
8_1^+	6_2^+	<14.5	20.2	4.6
8_1^+	6_1^+	<51.8	63.4	41.4
8_2^+	6_2^+	74 ± 40	46.6	32.4
8_2^+	6_1^+	9^{+9}_{-4}	10.7	2.2
10_1^+	8_1^+	<46.6	46.7	32.9
9_2^+	9_1^+	<39.4	11.8	11.7

TABLE IV. ^{48}Ti $M1$ transitions, $B(M1)$ in μ_n^2. See also caption to Table III.

J_n^π(i)	J_m^π(f)	Expt.	$(fp)^8$	$f^8(^{42}\mathrm{Sc})$
0_1^+	1_1^+	0.50 ± 0.08	0.54	0.73
0_1^+	1_2^+	0.50 ± 0.08	0.41	
0_1^+	1_5^+	0.80 ± 0.06	0.42	
2_2^+	2_1^+	0.5 ± 0.1	0.55	1.63
3_1^+	2_1^+	<0.01	0.55	1.63
3_1^+	4_1^+	<0.06	0.39	0.82
4_2^+	4_1^+	1.0 ± 0.2	1.78	3.45
2_3^+	2_1^+	0.05 ± 0.01	0.39	0.49
6_2^+	6_1^+	6.7 ± 3.3	2.32	8.96
6_3^+	6_1^+	0.9 ± 0.4	0.06	0.00
5_1^+	6_1^+	>0.36	0.41	1.00
5_2^+	6_2^+	>0.9	0.27	0.68
7_1^+	6_2^+	$0.09^{+0.09}_{-0.04}$	0.15	0.30
7_1^+	6_1^+	$0.14^{+0.14}_{-0.06}$	0.33	0.00
8_2^+	8_1^+	1.61 ± 0.70	1.59	3.38
7_2^+	8_1^+	$0.5^{+0.8}_{-0.2}$	0.82	0.00
7_2^+	6_1^+	$0.07^{+0.10}_{-0.03}$	0.12	0.57
9_1^+	8_2^+	>0.95	0.82	0.00
9_1^+	8_1^+	>0.36	0.57	1.55
8_3^+	7_1^+	$0.3^{+1.3}_{-0.1}$	0.54	1.09
8_3^+	8_1^+	$0.2^{+0.5}_{-0.1}$	0.25	0.00
10_2^+	9_1^+	$0.6^{+1.0}_{-0.3}$	3.60	7.08
11_1^+	10_2^+	>0.36	2.58	5.37
11_1^+	10_1^+	>0.36	0.81	0.00
12_1^+	11_1^+	0.5 ± 0.2	2.32	3.46

TABLE V. ^{48}Ti intrinsic quadrupole moments of the yrast states in e fm^2. $(fp)^8_s$ means Q_0 extracted from Eq. (14). $(fp)^8_t$ means Q_0 extracted from Eq. (15).

J_n^π(i)	$(fp)^8_s$	$f^8(^{42}\mathrm{Sc})$	$(f_{7/2}p_{3/2})^8$	$(fp)^8_t$
2_1^+	50.4	−12.25	39.17	68
4_1^+	32.18	−11.83	18.47	69
6_1^+	−44.25	13	13.99	
6_2^+	42	4	−25.18	42
8_1^+	32.54	1.67	31.52	44
10_1^+	46.69	13.34	30.29	37
12_1^+	35.78	28.58	31.64	
$Q_0(2^+)_{\mathrm{expt}} = 62 \pm 3$				

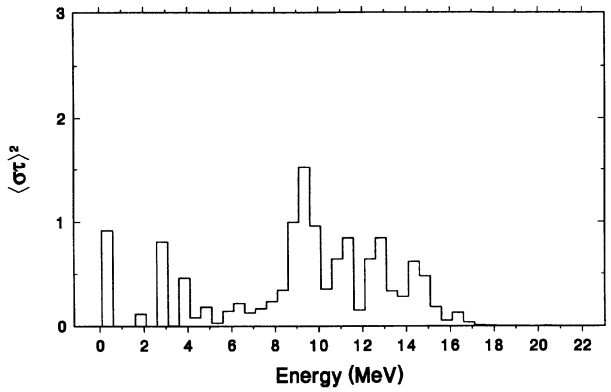

FIG. 4. ^{48}Ti → ^{48}V strength function. t=1 calculation.

similarity in gross structure: some low energy peaks, a resonancelike middle region, and $T = 2$ satellite strength higher up. In details they differ mainly in the position of the resonance, shifted down by some 2 MeV in the exact case. The total strength for the full space $S^- = 13.263\kappa^2$, combined with $S^+ = 1.263\kappa^2$ obtained for ^{48}Ti$(n,p)^{48}$Sc, satisfies the sum rule for the GT operator,

$$\sum B(\mathrm{GT}^-) - \sum B(\mathrm{GT}^+) = S^- - S^+ = 3(N-Z)\,\kappa^2. \tag{16}$$

As in the case of ^{48}Sc we show now the results for some truncations:

t_{parent}	t_{daughter}	GT$^-$	GT$^+$
0	1	15.44	3.44
1	2	14.44	2.44
2	3	13.71	1.71
3	4	13.46	1.46
Full	Full	13.26	1.26

The reduction of the GT$^+$ strength between MBZ and the result of the full calculation is even larger here. Again the $t_{\mathrm{parent}} = 3$ result is fairly close to the full one.

The mirror β^+ decay of ^{48}Fe to ^{48}Mn has $Q_{\mathrm{EC}} =$ 11.2 MeV, which covers a large fraction of the strength in Fig. 5. We have computed the half-life of ^{48}Fe and obtain

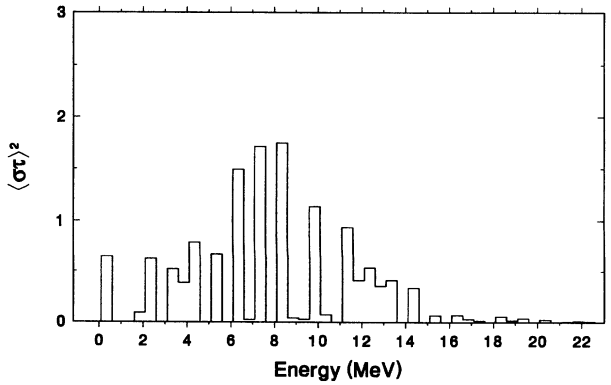

FIG. 5. ^{48}Ti → ^{48}V strength function. Full pf shell calculation.

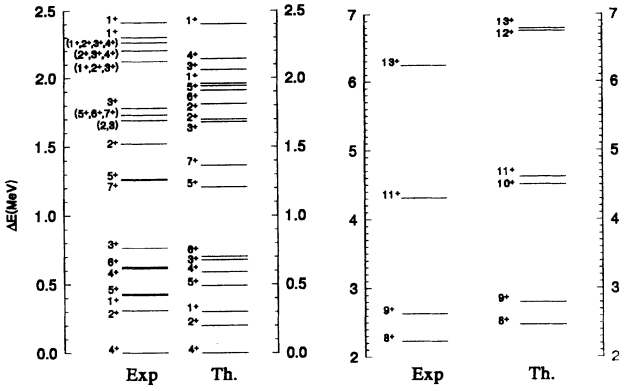

FIG. 6. Experimental and theoretical energy levels of ^{48}V.

$T_{1/2}$ = 36 ms, using the bare (g_A/g_V) for the Gamow-Teller decay and $T_{1/2}$ = 50 ms, if we use the effective value $0.77(g_A/g_V)_{\rm bare}$. In the first case the Fermi branch amounts to 33% while in the second it is 46%. An experimental comparison of the β^+ and (p,n) processes seems possible. It would certainly be welcome.

VI. ^{48}V, THE INTERACTION

In Fig. 6 we have plotted separately all levels with $J \leq 7$ below 2.5 MeV and the high spin ones. The claim that the agreement is excellent becomes repetitive.

The $M1$ and $E2$ transitions in Table VI show again excellent agreement. For the ground state, $\mu(4^+) = 1.90\mu_N$ against a measured $\mu(4^+) = 2.01\,(1)\mu_N$, while $\mu(2^+) = 0.51\mu_N$ against two measures $\mu(2^+) = 0.28\,(10)\mu_N$ and $0.444\,(16)\mu_N$ [35].

The Gamow-Teller β^+ decay to ^{48}Ti can reach J = 3, 4, and 5 daughter levels and three of them are fed as shown in Table VII. The resulting half-life $T_{1/2}$ = 8.85 d is almost half the observed one, $T_{1/2}$ = 15.97 d. The fraction of the total strength responsible for the decay is very small (0.4%). Therefore, the discrepancy in the half-lives could be cured by reducing by half the height of the lowest two bumps in Fig. 7, which is hardly a change in the overall picture.

TABLE VI. ^{48}V electromagnetic transitions, $B(E2)$ in e^2 fm^4 and $B(M1)$ in μ_N^2.

J_n^π(i)	J_m^π(f)	$B(E2)_{\rm expt}$	$B(E2)_{\rm theor}$
2_1^+	4_1^+	28.59(17)	48.1
5_1^+	4_1^+	104(42)	209.0
4_2^+	4_1^+	63(25)	28.9
4_2^+	5_1^+	<41	32.0
6_1^+	5_1^+	186(73)	191.0
6_1^+	4_1^+	46(6)	52.0
5_2^+	4_2^+	>176(124)	41.0
2_2^+	2_1^+	>1.3(19)	10.7
J_n^π(i)	J_m^π(f)	$B(M1)_{\rm expt}$	$B(M1)_{\rm theor}$
1_1^+	2_1^+	>0.027	3.12
5_1^+	4_1^+	0.081(14)	0.188
4_2^+	5_1^+	0.045(9)	0.032
4_2^+	4_1^+	0.0084(9)	0.0079
6_1^+	5_1^+	0.027(5)	0.027

TABLE VII. ^{48}V $(4^+) \rightarrow$ ^{48}Ti (J_f) beta decay.

J_f	$B({\rm GT})_{\rm theor}$	$B({\rm GT})_{\rm expt}$
4_1^+	$7.9\ 10^{-3}$	$4.1\ 10^{-3}$
3_1^+	$0.5\ 10^{-3}$	$1.7\ 10^{-3}$
4_2^+	$2.2\ 10^{-3}$	$4.1\ 10^{-3}$

As in the previous cases, we compare GT$^+$ and GT$^-$ for several t values:

$t_{\rm parent}$	$t_{\rm daughter}$	GT$^-$	GT$^+$
0	1	11.23	5.23
1	2	10.60	4.60
2	3	9.68	3.68
3	4	9.26	3.26
Full	Full	8.87	2.87

The reduction of the GT$^+$ strength between MBZ and the result of the full calculation is again of a factor of 2. The agreement between the $t_{\rm parent} = 3$ result and the full one begins to deteriorate.

Odd-odd nuclei provide a good test for the interactions and ^{48}V offers a good example of a general trend: Perturbative calculations [24] are quite good but the exact results come definitely closer to the data. This systematic improvement clearly indicates that the interaction is excellent. The one exception to the trend comes in ^{48}Sc, and is related to the choice of the KB3 (rather than KB1) interaction, as will be made clear in Sec. X.

VII. ^{48}Cr, ROTATIONAL MOTION

Some levels in ^{48}Cr are populated in the decay of ^{48}Mn and will be discussed in the next section. Beyond that, little is known of the spectrum, except the yrast line and before we come to it, we go through Fig. 8 for the strength

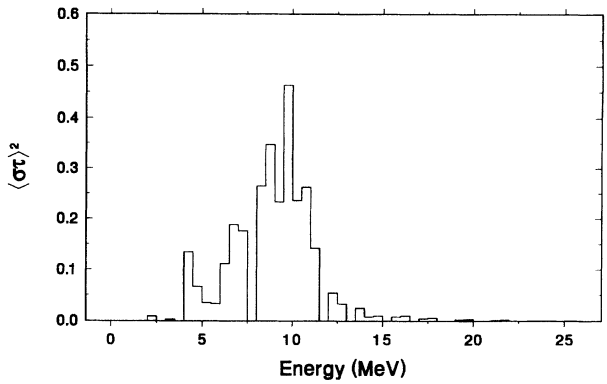

FIG. 7. Strength function for the ^{48}V beta decay. Full pf shell calculation.

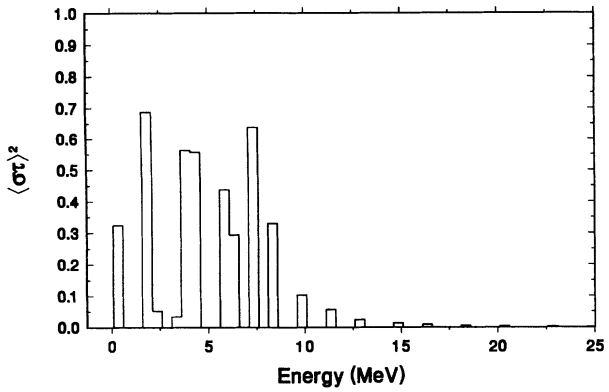

FIG. 8. ^{48}Cr $\rightarrow$ ^{48}V strength function. Full pf shell calculation.

function. Only the first 1^+ state is seen through the Q_β window. The calculated half-life is $T_{1/2} = 21.8$h and the observed one $T_{1/2} = 21.56\,(3)$ h.

The results for the truncations and the full calculations for GT$^+$ and GT$^-$ are now the following:

t_{parent}	t_{daughter}	GT$^-$	GT$^+$
0	1	7.66	7.66
1	2	6.94	6.94
2	3	5.64	5.64
3	4	5.17	5.17
Full	Full	4.13	4.13

The reduction of the GT$^+$ strength between MBZ and the result of the full calculation remains close to 2. The result of the full calculation is now 20% smaller than the $t_{\text{parent}} = 3$ result.

Table VIII and Fig. 9 collect the information about the yrast levels including the recently measured 12^+ and 14^+ [36]. The only complaint we may have with the data is the $B(E2, 8^+ \rightarrow 6^+)$ value but the calculations are telling us much more than that they agree with observations.

According to the criteria of constancy for Q_0 and $J(J+1)$ spacings defined in Sec. V we cannot speak of a *good* rotor yet, but we are coming close to it. The $J(J+1)$ behavior is at best incipient but the constancy of Q_0 is quite convincing. Furthermore if we plot the J values versus the energy of the emitted gammas (see Fig. 10) the experimental and the theoretical points follow the typical backbending pattern.

Two questions come naturally: What is the mechanism? Can we get better rotors?

TABLE VIII. Electromagnetic properties of the yrast band of ^{48}Cr, $B(E2)$ in e^2 fm^4, Q in e fm^2.

J	$B(E2, J \rightarrow J-2)$		Q_{spec}	Q_0	
	Expt.	Theor.		from Q_{spec}	from $B(E2)$
2	321 ± 41	228	−29.5	103	107
4	259 ± 83	312	−39.2	108	105
6	>161	311	−39.7	99	100
8	67 ± 23	285	−38.9	93	93
10	>35	201	−22.5	52	77
12		146	−5.3	12	

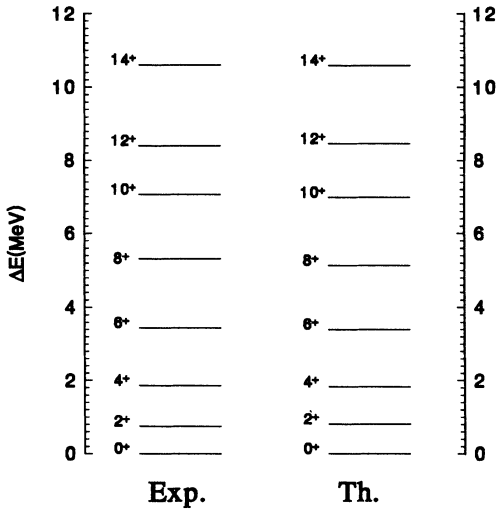

FIG. 9. Predicted and experimental Yrast band of ^{48}Cr.

Table V suggests that it is the mixing of $f_{7/2}$ and $p_{3/2}$ orbits that is at the origin of a well defined prolate intrinsic state. The hint is that of the two $\Delta j = 2$ sequences into which a major shell splits under the influence of the spin-orbit force (e.g., $g_{9/2}d_{5/2}s_{1/2}$ and $d_{3/2}g_{7/2}$), the lowest, at least, is efficient in producing quadrupole coherence that may lead to very good rotors. The hint has been taken up and the rotors that emerge are indeed very good, as will be shown in a future communication.

VIII. ^{48}Mn, TRUNCATIONS AND GT STRENGTH

Spectroscopically, ^{48}Mn is identical to ^{48}V (to within Coulomb effects). Its decay to ^{48}Cr covers a non-negligible fraction of the strength function [37,38]. Since this process and similar ones in the region have been analyzed so far with $t = 1$ calculations, we are going to compare them with $t = 3$ and exact ones. A digression may be of use.

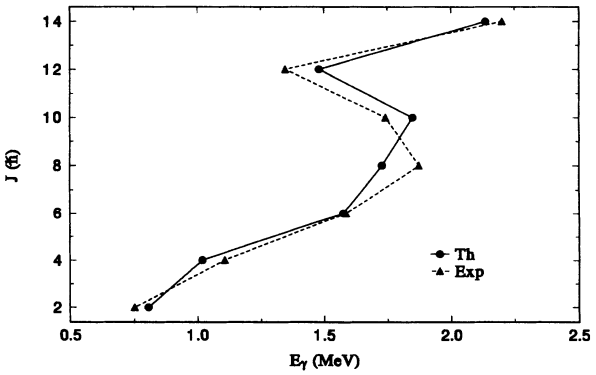

FIG. 10. Yrast band of ^{48}Cr.

TABLE IX. ^{48}Mn half-lives with different truncations compared with the experimental results.

Half-life (ms)	$t=1$	$t=3$	Full	Expt.
Total	99	133	142	158(22)
Partial Fermi	244	244	244	275(20)
Partial GT	107	292	340	372(20)
Total (theoretical energies)	41	80	116	

In a decay, the parent is basically an f^n state. Some daughters are also of f^n type but most are $f^{n-1}r$. In a $t=1$ calculation for the daughter, both configurations are present but f^n is allowed to mix with $f^{n-1}r$ through W_{fffr} matrix elements while $f^{n-1}r$ is not allowed to go to $f^{n-2}r^2$. At the $t=2$ level, pairing (i.e., W_{ffrr} matrix elements) comes in and pushes f^n down through mixing with $f^{n-2}r^2$, while $f^{n-1}r$ cannot benefit from a similar push from $f^{n-3}r^3$. It is only at the $t=3$ level that both f^n and $f^{n-1}r$ states can be treated on equal footing. This argument explains why a $t=2$ truncation for both parent and daughters is inconsistent but it does not guarantee that a $t=3$ truncation makes sense, unless the mixing is weak enough.

The results for the half life of ^{48}Mn are collected in Table IX. We see that the $t=3$ truncation is quite acceptable. For the total half-life the $t=1$ number is not too bad if we remember that full calculations are not always as accurate as they are here. However, this relatively good performance owes much to a strong Fermi branch: The partial GT value for $t=1$ is simply bad. The last line of Table IX gives an idea of the consequences of using calculated instead of observed energies for the transitions.

Next we move to the strength functions in Figs. 11, 12, and 13, where the experimental data show as dots. Globally the three calculations agree in that there is a resonance at $\sim$ 13 MeV and structure at $\sim$ 5 MeV. Beyond that, $t=3$ provides a fairly accurate view of the exact shape while $t=1$ does not. The values of the total GT$^+$ strength are the same as the GT$^-$ values in ^{48}V. To give an idea of the energetics, the 4^+ $T=1$ Isobaric Analog State (IAS) of the ^{48}Mn ground state is at 5.79 MeV in ^{48}Cr, $t=1$ puts it at 3.64 MeV, $t=3$ at 4.77 MeV, and the exact value is 5.38 MeV (not very good by our standards; see later in Sec. XI).

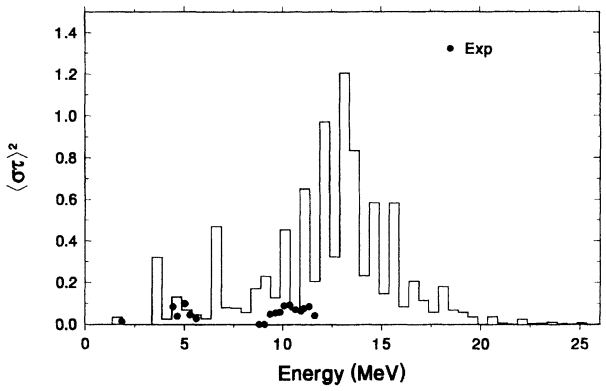

FIG. 12. ^{48}Mn $\rightarrow$ ^{48}Cr strength function. $t=3$ calculation.

Now we come to the data and concentrate on the exact calculation. Figure 14 contains very much the same information as Fig. 13 but instead of $\langle\sigma\tau\rangle^2$ we represent B(GT), affected by the $(0.77)^2$ quenching factor for the calculated numbers. Furthermore, between 6 and 8.5 MeV we have eliminated among these the peaks that fall below the observation threshold (shown as a dashed curve) [38].

At low energy, the peak at 2 MeV and the cluster of states centered at 5 MeV are very well positioned in the calculations that yield a strength of 0.50 in the interval [0,5.75] MeV against an observed 0.49. Between 5.75 and 8.75 MeV nothing is seen experimentally, and the only calculated strength above the sensitivity limit is located in two peaks in the [7.25,7.50] MeV bin. At these energies the calculated levels are not yet eigenstates of the system but doorways whose strength (0.41) will be fragmented (see next section).

Above 8.75 MeV observation resumes through delayed protons yielding B(GT)=1.07 in the [8.75,11.75] MeV in-

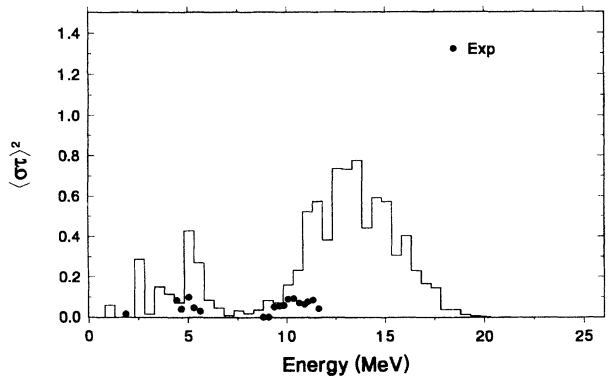

FIG. 11. ^{48}Mn $\rightarrow$ ^{48}Cr strength function. $t=1$ calculation.

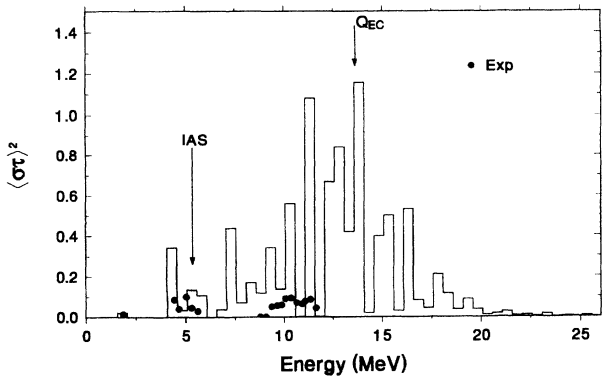

FIG. 13. ^{48}Mn $\rightarrow$ ^{48}Cr strength function. Full pf shell calculation.

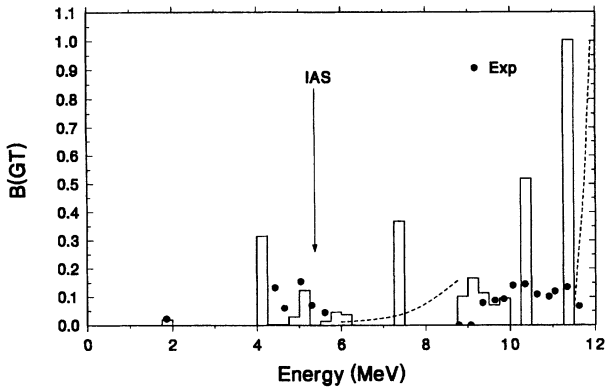

FIG. 14. Blowup of the low energy part of Fig. 13. Here we plot B(GT). Theoretical B(GT) values include standard $(0.77)^2$ quenching. Dotted lines show the observational thresholds [38]. Bins of 250 keV for the calculations (vs 500 keV in Figs. 10, 11, and 12).

terval versus the calculated 2.07 mostly found in two bins at [10.25,10.50] and [11.25,11.50] MeV. At these energies the density of levels is high and fragmentation will become important. Furthermore, half of the calculated strength is in the last bin, dangerously close to the abrupt rise in the sensitivity threshold. Therefore, before we conclude that experiments demand *anomalous* quenching (i.e., beyond the standard value) we shall analyze more closely what is being calculated and what is being measured.

IX. QUENCHING, SHIFTING, AND DILUTING GT STRENGTH

From all we have said about GT transitions, a broad trend emerges: Low lying levels are *very well* positioned and within minor discrepancies have the observed GT strength once standard quenching is applied. The examples of good energetics are particularly significant for the group around 5 MeV in ^{48}Cr and the 1^+ levels in ^{48}Ti (Fig. 3) and ^{48}Sc (Table II) that have experimental counterparts within 100 keV more often than not. The discrepancies are related to the shortish half-life of ^{48}Sc and ^{48}V, a slight lack of spin strength in the lowest states of ^{48}Ti [18], and—perhaps—with the tail of the resonant structure in ^{48}Cr discussed in the preceding section.

To cure the discrepancies we need a mechanism that may affect very slightly the overall GT distribution, without affecting the positions and other properties of the underlying levels, which are very well reproduced. Here, it is useful to be reminded how the strength function is obtained.

First, we define a state $|s\rangle$ by acting on the parent, $|s\rangle = \sigma\tau|i\rangle S^{-1/2}$, which exhausts by construction the sum rule $S = \langle i|(\sigma\tau)^2|i\rangle$, and then evaluate the amplitude of $|s\rangle$ in each daughter state by doing Lanczos interactions using $|s\rangle$ as a pivot [18]. The first iteration produces the centroid and variance of the strength function, $E_s = \langle s|H|s\rangle$ and $v_s = \langle s|H^2 - E_s^2|s\rangle$, respectively. As the number of iterations ν increases, the strength—originally concentrated at E_s—is fragmented into ν peaks. The lowest converge to exact eigenstates (with their exact share of the total sum rule) at the rate of roughly one every 6–10 iterations. Figure 15 is the high resolution version of Fig. 13 and shows the situation after 45 iterations for each of the JT values ($J = 3, 4, 5$; $T = 0, 1, 2$). It is only below approximately 6 MeV that we have a complete picture of the spectrum. Above, many thousand states are waiting to come and erode the strong peaks.

Let us examine first the global properties associated with S and E_s and then turn to the consequences of local fragmentation.

Quenching. Calculations always produce too much strength that has to be reduced by a quenching factor, which is the stronger (i.e., smaller) the most drastic the truncation [18]. For exact calculations in *one major shell* ($0\hbar\omega$), S has to be reduced by $(0.77)^2$, *which is very much the value demanded by the "violation" of the model-independent sum rule* (16). There is very little we can do *within a* $0\hbar\omega$ *calculation* to change this state of affairs.

Shifting. Contrary to S, which depends on geometry (16) and on overall properties of H, E_s may be significantly affected by small changes in the $\sigma\cdot\sigma$ and $\sigma\tau\cdot\sigma\tau$ contributions to H. In Ref. [39] it is shown that these spin-spin terms are very strong, especially the second, and may differ from force to force by some 20%. Therefore, the mechanism to cure the small discrepancies we have mentioned may well come from modifications in these components of the interaction that would produce small overall *shifts* of the distribution, and nothing else.

Now we return to the quenching problem. In view of discrepancies between (p, n) and β^+ data for ^{37}Ca, the extraction of S from the former has been recently criticized [40,41]. The problem was compounded by the fact that calculations with Wildenthal's W interaction suggested that standard quenching did not seem necessary. However, Brown's analysis [42] indicates that this effect may be due to a defect of the interaction. It is very interesting to note that what is called $12.5p$ in [42] is none other than KB, while CW—which gives the best results—is very basically a minimally modified KB that

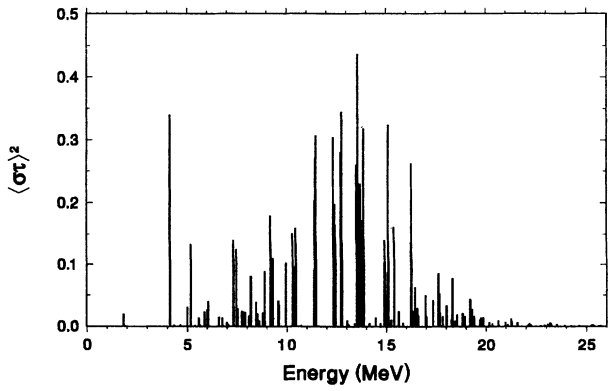

FIG. 15. Same as Fig. 13 but without binning.

can be safely assimilated to KB1 or KB3.

Diluting. Brown's analysis contains another important hint: Once normalized by the $(0.77)^2$ factor, the CW calculations follow smoothly the data within the β window, but then produce too much strength when compared with the (p,n) reaction. The suggestion from Fig. 15 is that in regions where the density of levels becomes high, fragmentation may become so strong that much strength will be so *diluted* as to be rendered unobservable. The difference between the A=37 and A=48 spectra is that in the former the effect is almost exclusively due to intruders, while in the latter the density of pf states is high enough to produce substantial dilution by itself, which brings us back to the problem of the amount of strength calculated between 8.75 and 11.75 MeV in ^{48}Cr, double the measured value. Some shifting may be warranted to reduce the discrepancy, but Fig. 15 suggests very strongly that dilution be made responsible for it (i.e., for anomalous quenching).

From all this, it follows that simultaneous measurements of β^+ and (p,n) strength are very much welcome in pairs of conjugate nuclei where the β^+ release energy is large, the $0\hbar\omega$ spectrum is dense, and high quality calculations are feasible. We propose the following candidates for which the calculations are already available:

β^+	(p,n)
^{45}Cr $\rightarrow$ ^{45}V	^{45}Sc $\rightarrow$ ^{45}Ti
^{46}Cr $\rightarrow$ ^{46}V	^{46}Ti $\rightarrow$ ^{46}V
^{47}Mn $\rightarrow$ ^{47}Cr	^{47}Ti $\rightarrow$ ^{47}V
^{48}Fe $\rightarrow$ ^{48}Mn	^{48}Ti $\rightarrow$ ^{48}V.

To conclude, a theoretical understanding of standard quenching demands that we look at the full wave function and not only at its $0\hbar\omega$ components. Experimentally, what has to be explained is the disappearance of strength, i.e., standard *and* anomalous quenching (as observed in ^{48}Cr). Dilution will no doubt play a role in both, but the latter may be observed already by comparisons with $0\hbar\omega$ calculations.

X. VALIDITY OF MONOPOLE MODIFIED REALISTIC INTERACTIONS

To answer with some care the question raised in the Introduction we review briefly the work related to monopole corrections.

The first attempt to transpose the results of Refs. [5,6] to the *sd* shell met with the problem that the interaction had to evolve from ^{16}O to ^{40}Ca. A linear evolution was assumed, but it was shown that the centroids followed more complicated laws demanding an excessive number of parameters [43].

The solution came in Ref. [44], by adopting a hierarchy of centroids and noting that the realistic matrix elements depend on the harmonic oscillator frequency very much as

$$W^{JT}_{rstu}(\omega) = \frac{\omega}{\omega_0} W^{JT}_{rstu}(\omega_0), \tag{17}$$

thus displacing the problem of evolution of H to one of evolution of ω. The classical estimate $\hbar\omega = 40A^{-1/3}$ [45] relies on filling oscillator orbits and on adopting the $r = r_0 A^{1/3}$ law for radii, which nuclei in the p and *sd* shells do not follow. Therefore it was decided to treat ω as a free parameter for each mass number and then check that the corresponding oscillator orbits reproduce the observed radii. This turned out to work very well and to produce very good spectroscopy in all regions where exact calculations could be done.

The method relies on the rigorous decomposition of the full Hamiltonian as $\mathcal{H} = \mathcal{H}_m + \mathcal{H}_M$, where the monopole part $\mathcal{H}_m$ is responsible for saturation properties, while $\mathcal{H}_M$ contains all the other multipoles. Upon reduction to a model H, $\mathcal{H}_m$ is represented by H_m, which contains the binding energies of the closed shells, the single-particle energies, and the centroids. Everything else goes to H_M, which nevertheless depends on $\mathcal{H}_m$ through the orbits, in principle self-consistently extracted from $\mathcal{H}_m$ [44,39,46]. The program of minimal modifications now amounts to discarding from the nucleon-nucleon potential the $\mathcal{H}_m$ part and accepting all the rest, unless some irrefutable arguments show up for modifying something else. On the contrary $\mathcal{H}_m$ is assumed to be purely phenomenological and the information necessary to construct it comes mostly from masses and single-particle energies [46].

The proof of the validity of the realistic $\mathcal{H}_M$ through shell model calculations depends on the quality of the monopole corrections. In some regions we may have to go beyond the oscillator approximation. In particular, at the beginning of the *sd* shell the observed radii have a complicated behavior that can be reproduced practically within error bars by Hartree-Fock calculations with Skyrme forces with orbital fillings extracted from the shell model wave functions [47]. Obviously the $d_{5/2}$, $s_{1/2}$, and $d_{3/2}$ orbits are poorly reproduced by a single ω, and obviously this makes a difference in the two-body matrix elements [48] (work is under progress on this problem).

Therefore, in the *sd* shell—to match or better the energy agreements obtained with Wildenthal's W (or USD) interaction [49,50]—we have to push a bit further the work of Ref. [44].

When we move to the pf shell, no such efforts are, or were, necessary. Because of $f_{7/2}$ dominance, it is much easier to determine the centroids: The V^T_{rr} values are no issue, the crucial V^T_{fr} ones can be read (almost) directly from single-particle properties on ^{49}Ca and ^{57}Ni, and we are left with V^T_{ff}, only two numbers. Once we have good enough approximations for the centroids we can do shell model calculations to see how the rest of H (i.e., H_M) behaves. In Ref. [24] it was found that H_M behaves quite well, but much better in the second half of the f^n region: A=48 happens to be the border beyond which quite well becomes very well. Hence the remark in the second paragraph of the Introduction.

The trouble at the beginning of the region was attributed at the time to intruders, but now we know that radial behavior must be granted its share. It is here that KB3 comes in. Although Eq. (5) has only cosmetic effects, its origin is not cosmetic: It was meant to simulate

necessary corrective action *not related to the presence of intruders*. It reflects the fact that in the neighborhood of ^{40}Ca the interaction works better if the spectrum of ^{42}Sc is better reproduced, while at $A=48$ and after, the KB interaction—not very good in ^{42}Sc—needs no help, except in the centroids, as we have shown.

Most probably this says something about radial behavior at the beginning of the region. It is poorly known except in the Ca isotopes, where it is highly nontrivial [51]. The indications are that when shell model calculations demand individual variations of matrix elements in going from nucleus to nucleus the most likely culprits are the single-particle orbits. And the indications are that at $A=48$ the need for such considerations disappears: As we have mentioned at the beginning of Sec. IV (^{48}Sc) and the end of Sec. VI (^{48}V), it is only in ^{48}Sc—which is most sensitive to the KB3 modifications—that the exact calculations are not definitely better than earlier approximate ones.

It is from these indications that we conclude that we would have done just as well or better with KB1, but the differences with respect to KB3 are too small to justify redoing all the calculations. The general statement is that monopole corrected realistic interactions are the ones that *should* be used in calculations, keeping in mind that in some regions the corrections may demand some extra care.

XI. NOTE ON BINDING ENERGIES

Our interaction overbinds all the $A=48$ nuclei by about the same amount, indicating the need of small corrections in the centroids. A constant shift of 780 keV, whose origin may be related to residual monopole defects (probably a tiny mass dependence of the effective interaction), leads to the binding energies relative to ^{40}Ca collected in Table X. The Coulomb energies are calculated using the following expressions ($n = \pi + \nu, \pi$ = protons, ν = neutrons) [5]:

$$H_{\mathrm{Coul}} = V_{\pi\pi}\pi(\pi-1)/2 + V_{\pi\nu}\pi\nu + 7.279\pi \text{ MeV},$$
$$V_{\pi\pi} = 0.300(50) \text{ MeV}, V_{\pi\nu} = -0.065(15) \text{ MeV}. \quad (18)$$

For ^{48}Fe we obtain BE=43.19 MeV, leading to a decay energy of $Q_{\mathrm{EC}} = 11.23$ MeV for $^{48}\mathrm{Fe} \rightarrow {}^{48}\mathrm{Mn}$. The most recent estimate of Audi and Wapstra [52] gives BE(^{48}Fe) = 43.14 MeV and $Q_{\mathrm{EC}} = 11.18$ MeV. The precision of the calculated Coulomb energies can be checked [17] through the position of the analog of ^{48}V in ^{48}Cr, experimentally at 5.79 MeV against the Coulomb corrected value of 5.68 MeV that can be obtained from Table X. As noted in Sec. VIII, for this state there is a 400 keV discrepancy between experiment and calculation, high by our standards. It probably indicates the need of some more sophistication in the readjustment of monopole terms than the shift we have suggested. Note that the theory-experiment differences in Table X are typical of the results throughout the paper.

TABLE X. Binding energies relative to ^{40}Ca (MeV), $A=48$.

	Ca	Sc	Ti	V	Cr	Mn	Fe
Expt.	73.94	73.44	76.65	71.85	69.41	55.10	43.14
Theor.	74.00	73.41	76.58	71.89	69.13	55.20	43.19

XII. CONCLUSIONS

Since much of Secs. IX and X was devoted to drawing conclusions about the two main problems addressed, we shall only sum them up:

(i) The detailed agreement with the data lends strong support to the claim that minimally monopole modified realistic forces are the natural and correct choice in structure calculations.

(ii) The description of Gamow-Teller strength is quite consistent with the data, to within the standard quenching factor. The calculations strongly suggest that dilution due to fragmentation makes much of the strength unobservable.

Two by-products emerge from the calculations. The first is mainly technical:

(iii) Truncations at the $t = 3$ level are reasonable in the lower part of the *pf* shell for level schemes and global trends of the strength functions. As shown by the GT$^+$ results care has to be taken when they are used in the calculation of other observables.

The second by-product is more interesting:

(iv) The calculations provide insight into the notion of intrinsic states and suggest a mechanism to produce rotational motion in a shell model framework.

ACKNOWLEDGMENTS

This work has been supported in part by the DGICYT (Spain) Grant No. PB89-164 and by the IN2P3 (France)-CICYT (Spain) agreements.

[1] G.F. Bertsch and H. Esbensen, Rep. Prog. Phys. **50**, 607 (1987).
[2] J.N. Ginocchio and J.B. French, Phys. Lett. **7**, 137 (1963); J. N. Ginocchio, Phys. Rev. **144**, 952 (1966).
[3] J.D. Mc Cullen, B.F. Bayman, and L. Zamick, Phys. Rev. **4**, B515 (1964).
[4] H. Horie and K. Ogawa, Nucl. Phys. **A216**, 407 (1973).
[5] E. Pasquini, Ph.D. thesis, Report No. CRN/PT 76-14, Strasburg, 1976.
[6] E. Pasquini and A.P. Zuker, in *Physics of Medium Light*

Nuclei, Florence, 1977, edited by P. Blasi and R. Ricci (Editrice Compositrice, Bologna, 1978).
[7] A.G.M. van Hess and P.W.M. Glaudemans, Z. Phys. A **303**, 267 (1981).
[8] R.B.M. Mooy and P.W.M. Glaudemans, Z. Phys. A **312**, 59 (1983).
[9] R.B.M. Mooy and P.W.M. Glaudemans, Nucl. Phys. **A438**, 461 (1985).
[10] K. Muto and H. Horie, Phys. Lett. **138B**, 9 (1984).
[11] A. Yokohama and H. Horie, Phys. Rev. C **31**, 1012 (1985).
[12] K. Muto, Nucl. Phys. **A451**, 481 (1986).
[13] J.B. Mc Grory, B.H. Wildenthal, and E.C. Halbert, Phys. Rev. C **2**, 186 (1970).
[14] J.B. Mc Grory and B.H. Wildenthal, Phys. Lett. **103B**, 173 (1981).
[15] J.B. Mc Grory, Phys. Rev. C **8**, 693 (1973).
[16] B.J. Cole, J. Phys. G **11**, 481 (1985).
[17] W.A. Richter, M.G. Van der Merwe, R.E. Julies, and B.A. Brown, Nucl. Phys. **A523**, 325 (1991).
[18] E. Caurier, A. Poves, and A.P. Zuker, Phys. Lett. B **256**, 301 (1991).
[19] K. Ogawa and H. Horie, in *Nuclear Weak Processes and Nuclear Structure*, edited by M. Morita *et al.* (World Scientific, Singapore, 1990).
[20] E. Caurier, A. Poves, and A.P. Zuker, Phys. Lett. B **252**, 13 (1990).
[21] J. Engel, W.C. Haxton, and P. Vogel, Phys. Rev. C **46**, 2153 (1992).
[22] W. Kutschera, B.A. Brown, and K. Ogawa, Riv. Nuovo Cimento **1**, 12 (1978).
[23] A. Poves, E. Pasquini, and A.P. Zuker, Phys. Lett. **82B**, 319 (1979).
[24] A. Poves and A.P. Zuker, Phys. Rep. **70**, 235 (1981).
[25] T.W. Burrows, Nucl. Data Sheets **68**, 1 (1993).
[26] E. Caurier, computer code ANTOINE, CRN, Strasburg, 1989.
[27] E. Caurier, A. Poves, and A.P. Zuker, in *Nuclear Structure of Light Nuclei far from Stability. Experiment and Theory*, Proceedings of the Workshop, Obernai, edited by G. Klotz (CRN, Strasburg, 1989).
[28] R.R. Whitehead, in *Moment Methods in Many Fermion Systems*, edited by B.J. Dalton *et al.* (Plenum, New York, 1980).
[29] S.D. Bloom and G.M. Fuller, Nucl. Phys. **A440**, 511 (1985).
[30] T.T.S. Kuo and G.E. Brown, Nucl. Phys. **A114**, 241 (1968).
[31] A.R. Edmonds, *Angular Momentum in Quantum Mechanics* (Princeton University Press, Princeton, 1960).
[32] D.H. Wilkinson and B.E.F. Macefield, Nucl. Phys. **A232**, 58 (1974).
[33] W. Bambynek, H. Behrens, M.H. Chen, B. Graseman, M.L. Fitzpatrick, K.W.D. Ledingham, H. Genz, M. Mutterer, and R.L. Intemann, Rev. Mod. Phys. **49**, 77 (1977).
[34] D.G. Fleming, O. Nathan, H.B. Jensen, and O. Hansen, Phys. Rev. C **5**, 1365 (1972).
[35] P. Raghavan, At. Data Nucl. Data Tables **42**, 189 (1989).
[36] J.A. Cameron, M.A. Bentley, A.M. Bruce, R.A. Cunningham, H.G. Price, J. Simpson, D.D. Warner, A.N. James, W. Gelletly, and P. Van Isacker, Phys. Lett. B **319**, 58 (1993).
[37] T. Sekine, J. Cerny, R. Kirchner, O. Klepper, V.T. Koslowsky, A. Plochocki, E. Roeckl, D. Schardt, B. Shenill, and B.A. Brown, Nucl. Phys. **A467**, 93 (1987).
[38] J. Szerypo, D. Bazin, B.A. Brown, D. Guillemaud-Muller, H. Keller, R. Kirchner, O. Klepper, D. Morrissey, E. Roeckl, D. Schardt, and B. Sherrill, Nucl. Phys. **A528**, 203 (1991).
[39] M. Dufour and A.P. Zuker, Centre de Recherches Nucléaires de Strasbourg Report No. CRN 93-29, 1993.
[40] E.G. Adelberger, A. Garcia, P.V. Magnus, and D.P. Wells, Phys. Rev. Lett. **67**, 3658 (1991).
[41] M.B. Aufderheide, S.D. Bloom, D.A. Resler, and D.C. Goodman, Phys. Rev. C **46**, 2251 (1992).
[42] B.A. Brown, Phys. Rev. Lett. **69**, 1034 (1992).
[43] A. Cortés and A.P. Zuker, Phys. Lett. **84B**, 25 (1979).
[44] A. Abzouzi, E. Caurier, and A.P. Zuker, Phys. Rev. Lett. **66**, 1134 (1991).
[45] A. Bohr and B. Mottelson, *Nuclear Structure* (Benjamin, New York, 1969).
[46] A.P. Zuker, Nucl. Phys. (in press).
[47] A. Abzouzi, J.M. Gomez, C. Prieto, and A.P. Zuker, Centre de Recherches Nucléaires de Strasbourg Annual Report, 1990, p. 15.
[48] S. Kahana, H.C. Lee, and C.K. Scott, Phys. Rev. **180**, 956 (1969).
[49] B.H. Wildenthal, Prog. Part. Nucl. Phys. **11**, 5 (1984).
[50] B.A. Brown and B.H. Wildenthal, Annu. Rev. Nucl. Part. Sci. **38**, 292 (1988).
[51] E. Caurier, A. Poves, and A.P. Zuker, Phys. Lett. **96B**, 15 (1980).
[52] G. Audi and A.H. Wapstra, Nucl. Phys. **A565**, 1 (1993).